

TOWARDS A HIGH THROUGHPUT SOLUTION FOR BORON-OXYGEN RELATED REGENERATION

Axel Herguth, Giso Hahn

University of Konstanz, Department of Physics, 78457 Konstanz, Germany

ABSTRACT: Boron-oxygen related defects are a serious problem limiting the efficiency of solar cells based on boron-doped silicon. But even though the regeneration (a.k.a. permanent deactivation) of BO-related defects was introduced in 2006, it is still limited mainly to laboratory use and almost always illumination is used to induce the regeneration process. In this contribution external biasing/current injection is used to trigger the regeneration effect. The regeneration process itself is carried out in a stack of solar cells optionally separated by conductive spacers. In this configuration a multitude of solar cells can be treated simultaneously. In addition to inducing the regeneration process the external biasing brings along electrical losses and thus heats up the stack. This self-heating can be used to reach and/or hold the temperature required for the regeneration process. For high current densities an active regulation of temperature is necessary. The working principle could be successfully proven. **Keywords:** boron-oxygen related defects, degradation, industrial implementation

1 INTRODUCTION

Boron-oxygen related defects can have a devastating influence on the minority carrier lifetime in boron-doped oxygen-rich silicon [1]. Within few hours of carrier injection (either by light or by external biasing) the initially inactive defect (annealed state, Fig. 1) evolves to an extremely recombination active defect (degraded state, Fig. 1) reducing the lifetime and thus the efficiency of affected solar cells. As the defect concentration scales almost quadratically with the interstitial oxygen concentration in the material [1,2], this effect mainly affects monocrystalline oxygen-rich Czochralski-grown (Cz) silicon material.

In 2006, Herguth *et al.* have shown that the recombination active form of the defect (degraded state) can be converted into a third, inactive form (regenerated state, Fig. 1) at slightly elevated temperatures and carrier injection either by light or by external biasing [3,4] restoring permanently the full efficiency potential of boron-doped solar cells. Therefore, the so called regeneration process a.k.a. permanent deactivation of BO-related defects should be – in principle – a process of high relevance to industrial processing of Cz-Si material.

However, even though the process is nowadays often used for lab-type or prototype solar cells, the integration into industrial mass production has not been shown yet.

In this contribution the differences between lab-type application and mass production issues will be discussed and a promising concept will be presented.

2 GENERAL CONSIDERATIONS

Degradation and regeneration may be described in a three state model according to Fig. 1 [6]. In principle, only two parameters can be accessed to manipulate the underlying defect in a given sample: temperature and carrier injection (either by light or by external biasing). There are other factors influencing the kinetics of the regeneration process as well. Most of these factors concern the manufacturing process, e.g., thermal history, but almost always the manufacturing process is defined by other constraints rather than a good regeneration behavior.

Carrier injection is essential for degradation and even more important for regeneration. While the degradation rate saturates already at an injection level around 1/100 suns [5], the regeneration rate still increases above 1 sun illumination or comparable external biasing [6].

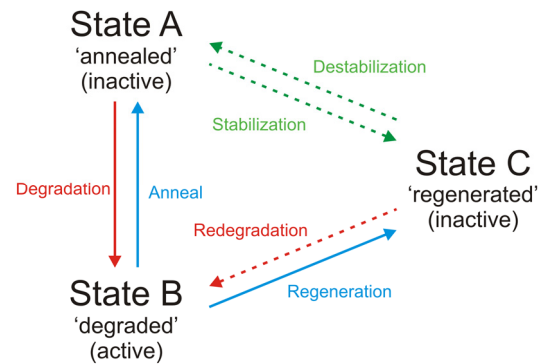


Figure 1: Definitions of defect states as well as possible reactions and typical conditions (adapted from [6]).

Temperature has a strong influence on the defect conversion rates [7,8]. In principle, a rising temperature shortens the time constants (\sim inverse rate) but individual reaction constants benefit differently. Especially the destabilization (Fig. 1) as undesired competitive reaction to the regeneration has to be taken into account. If the regeneration rate becomes too small compared to the destabilization rate, the equilibrium (reached for long treatment times) features a mixture of all defect states or even mostly shifts away from the regenerated state as depicted in Fig. 2. Therefore, the slower the regeneration rate the lower is the threshold temperature to achieve an almost complete conversion of defect states.

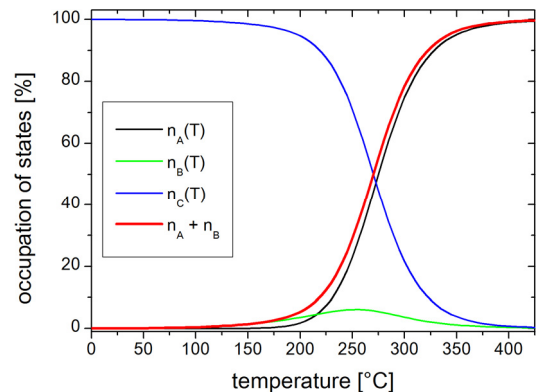


Figure 2: Occupation of the different defect states (see Fig. 1) in equilibrium versus temperature. The equilibrium shifts generally with temperature away from the regenerated state C, the exact values may deviate as they depend on the actual regeneration conditions [6].

3 LAB-TYPE APPLICATION

Usually, illumination is used for carrier injection in a laboratory environment as it is a relatively simple setup consisting roughly of a lamp and a heating/cooling stage. Very often lifetime samples are used, so that illumination is the only possibility to generate excess charge carriers. The spectrum of the light source is not very relevant as long as enough excess charge carriers are generated in the silicon bulk. The effectiveness and spatial homogeneity of the illumination is rarely of interest for the application to individual samples, and often only a fraction of the emitted light actually impacts on the sample. Even the exact duration of illumination is often irrelevant as long as the sample reaches completely the regenerated state.

Although this kind of setup is well suited for laboratory use, upscaling this method for industrial application with a multitude of samples will most probably exceed the limits of feasibility.

Applying the regeneration process as an add-on to the ‘normal’ manufacturing process means that each solar cell has to be heated and illuminated individually. This obviously needs space and, even assuming that the complete regeneration process takes only a couple of minutes, this may add up significantly.

Each solar cell requires illumination with certain intensity. Assuming a white light intensity of around 1 sun (100 mW/cm²), each 6” solar cell would require 25 W of optical power and around 125 W of electrical power (assuming an electrical-to-optical efficiency of 20%). In this consideration light missing the solar cells is ignored. The needed electrical power for the illumination would probably even exceed 150 W per solar cell. However, more intensity speeds up the process and more optical power is advisable, so the aforementioned 150 W should probably be considered a lower limit.

In the end, all comes down to the characteristic time constant of the asymptotic regeneration process, and one should keep in mind that a three- or fourfold time (maybe more) is required for complete regeneration.

4 TOWARDS INDUSTRIAL APPLICATION

Therefore, we propose a different approach using external biasing instead of illumination to trigger the regeneration process. Of course each cell has to be contacted on both polarities. But apart from that, external biasing offers promising features. First, the electrical efficiency should be by far higher than for optical implementation as electrical-to-optical conversion losses fall away. This will be discussed in the end in more detail. Secondly, the solar cells may be packed without the geometrical constraints of a light source thus a purely electrical implementation could feature a smaller footprint, especially in the setup presented hereafter.

4.1 Experimental setup

In our setup the solar cells are not treated sequentially but in form of a stack enclosed by electrodes as shown in Fig. 3. In such a way, the solar cells are connected in series and the contact to each polarity of the solar cell is given by the opposite polarity of the adjacent solar cell. Even though the expression ‘stack’ implies a vertical arrangement of the solar cells, it can be advantageous to use a horizontal arrangement as the weight of the solar cells and electrode above might damage a solar cell.

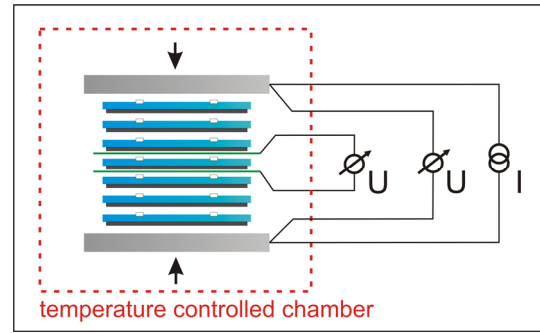


Figure 3: Setup used for the regeneration treatment. The solar cells are stacked between two electrodes optionally with conductive spacers between the solar cells. The electrodes are connected to an adjustable electrical power supply. The voltage of an individual solar cell in the stack can be measured by inserting a thin conductive (Al) foil. The setup is placed in a temperature controlled chamber allowing for heating or cooling. A temperature monitoring is mandatory.

Furthermore, it also can be beneficial to insert conductive spacers between the solar cells for two reasons. First, the filigree structures of the textured front surface as well as the contacts might be damaged by the back side of the adjacent solar cell, especially if lateral movement occurs. Secondly, it facilitates the circulation of air or other gases between the solar cells allowing for a temperature regulation. The cooling issue is addressed in section 4.4 in more detail. A proper monitoring and control of temperature is mandatory, hence the stack is isolated in a temperature controlled chamber.

4.2 A proof-of-principle experiment

In a first experiment 50 solar cells (1-3 Ωcm, 5” sq. Cz-Si, ~250 μm thick) were used. It was proven before the experiment that the solar cells degrade and regenerate. A single solar cell in the centre of the stack is wired so that an in-situ voltage measurement is possible. A relatively low constant current (~7 mA/cm²) was chosen, and the stack was preheated to 70°C prior to the experiment rendering automatically all boron-oxygen related defects in the annealed state. The applied voltage of the whole stack and the wired solar cell (placed in the centre) was continuously monitored and the results are depicted in Fig. 4.

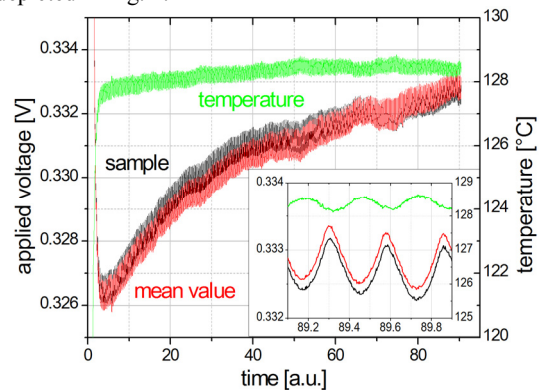


Figure 4: In-situ voltage measurement of the individually contacted solar cell and mean solar cell voltage in the stack during the regeneration treatment at ~130°C. The noisy appearance results from thermal oscillations induced by the heating source of the chamber shown in the inset.

In the beginning, the abrupt inset of the current or rather the dissipated power causes a strong rise of the temperature from $\sim 70^\circ\text{C}$ to $\sim 128^\circ\text{C}$. This brings the stack into a temperature range that is required for regeneration. As expected, the voltage dropout across the stack (reduced to a mean voltage for each solar cell) breaks down with temperature. The almost negligible difference between the mean solar cell voltage and the wired sample in the centre of the stack shows that the temperature distribution is almost homogenous in the stack. Even small differences in temperature would be recognizable as the voltage is very sensitive to temperature (using a constant current). This can be seen in the inset of Fig. 4 indicating that small temperature oscillations of $\sim 0.5\text{ K}$ yield an oscillation of the applied voltage of $\sim 1\text{ mV}$.

As temperature more or less stabilizes, the voltage shows a further increase of around 7 mV (at $\sim 130^\circ\text{C}$) due to the intended regeneration. This is far beyond fluctuation due to remaining temperature changes of the still active heating source of the chamber as can be seen in the inset of Fig. 4.

Only because of this temperature stabilization the ongoing regeneration process could be monitored in-situ. For this reason the weak biasing was chosen, which is rather hindering than beneficial with respect to the expected time constant.

After the experiment was stopped, the samples were intentionally exposed to degradation conditions ($< 50^\circ\text{C}$, low current) in order to reveal the fraction of non-regenerated defects. Afterwards V_{oc} under standard test conditions (STC) was compared to the annealed state prior to the experiment in order to evaluate whether the regeneration process was successful. The results are shown in Fig. 5. The observed loss of $\sim 2\text{ mV}$ in V_{oc} was somehow expectable as the applied voltages shown in Fig. 4 were still increasing when the experiment was stopped. Thus the regeneration was obviously not complete at that time. In addition, the observed 7 mV increase in voltage at $\sim 130^\circ\text{C}$ in Fig. 4 compared to the expected $10\text{--}12\text{ mV}$ in V_{oc} (determined on non-regenerated parallel samples at STC, blue zone in Fig. 5) points also towards an incomplete regeneration process. However, the average loss in V_{oc} of $\sim 2\text{ mV}$ after regeneration is small compared to the expectable drop in V_{oc} of $10\text{--}12\text{ mV}$ due to complete degradation. In respect thereof, the experiment acts as a proof-of-principle for a feasible high throughput regeneration procedure.

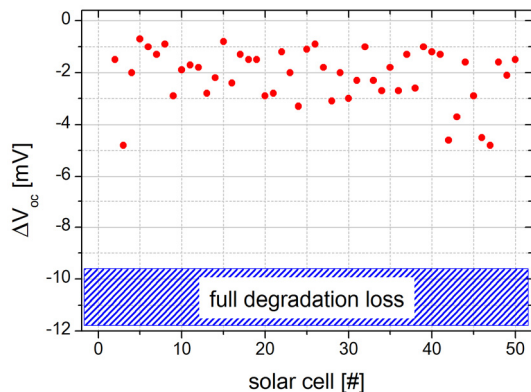


Figure 5: Difference of V_{oc} between annealed state prior to the regeneration treatment and the degraded state (after the regeneration process stopped) under STC. The blue region indicates the expected loss due to pure degradation determined on parallel samples.

4.3 Simulations

In the presented proof-of-principle experiment the stack was heated to 70°C prior to the inset of external biasing. But after a while the temperature had increased quite significantly due to electrical losses in the stack of solar cells even though a relatively low current was applied. For higher currents a stronger self-heating of the stack is expectable and indeed observed (not shown here) even though the system features a weak negative feedback mechanism as the dissipated power $P = V \cdot I$ is determined by the used constant current as well as the voltage of the stack which strongly drops with rising temperature.

An exemplary simulated temperature profile with time is shown in Fig. 6 (and Fig. 7) using a current density of 75 mA/cm^2 (\sim doubled j_{sc}) far larger than in the first experiment. The negative feedback mechanism is responsible for the deviation from a straight line. Within a minute the stack reaches the temperature range required for the regeneration process. The complete degradation-regeneration cycle occurs while the temperature is still increasing with a rate of around 1 K/s . This corresponds to a voltage drop rate of approximately 2 mV/s which conceals almost entirely any changes in applied voltage induced by the ongoing degradation-regeneration cycle, and thus in-situ monitoring becomes virtually impossible.

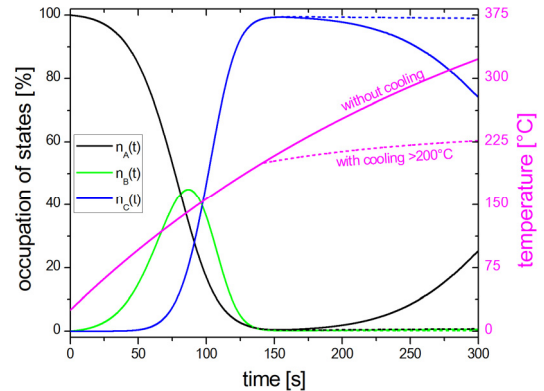


Figure 6: Exemplary simulation of the solar cell temperature profile resulting from power dissipation due to a constant current density of 75 mA/cm^2 and optional cooling for temperatures exceeding 200°C . Also shown is the occupation of states as reaction to the treatment. In this case a rather high regeneration rate was assumed.

Also shown in Fig. 6 and Fig. 7 is the occupation of the different states calculated using the set of coupled differential equations published earlier [8].

As starting condition the system was assumed to be completely in the annealed state A. However, using the degraded state B as starting condition, results more or less in the same curves of the regenerated state C.

The reaction constants according to Fig. 1 were parameterized with regard to temperature using the Arrhenius law. The used values for activation energy E_a and frequency prefactor are shown in Table I. The regeneration rate differs from the other rates as it seems to depend not only on temperature and injection but also on the process history of the sample.

Therefore, the result of the simulation shown in Fig. 6 differs from the one shown in Fig. 7 as a rather high and a rather low regeneration prefactor was used, respectively.

Table I: Simulation parameters

	E_a (eV)	ν (Hz)	
Anneal	1.32	$1 \cdot 10^{13}$	[7]
Degradation	0.44	$1 \cdot 10^4$	[7]
Regeneration (slow)	0.64	$2 \cdot 10^5$	[6]
Regeneration (fast)	0.64	$2 \cdot 10^6$	[6]
Destabilization	1.00	$2 \cdot 10^7$	[6]

It should be noted here that the used values are afflicted with uncertainty and values from literature exhibit some spreading. There might be deviations from Arrhenius' law as well, so the actual occupation of states in the experiment might differ from the calculated one. Nevertheless, Fig. 6 and Fig. 7 shall demonstrate two fundamentally different cases.

In the simulation with high regeneration rate depicted in Fig. 6 boron-oxygen related defects first move from the annealed state (black) via the degraded state (green) to the regenerated state (blue). In this case, an almost complete regeneration (meaning full occupation of the regenerated state) is reached after roughly 150 seconds. This would be the right time to stop the procedure.

But as the temperature without active cooling is still rising the phenomenon depicted in Fig. 2 gains in importance and the regenerated state becomes more and more instable. Thus, there is only a small process window in which a complete regeneration is achieved.

However, Fig. 6 also shows that this effect can be efficiently suppressed if the temperature can be stabilized or its increase is at least slowed down sufficiently. Thus the process window may be widely extended making the whole process less prone to failure.

If the regeneration rate is comparably small (in this case only a tenth of the previously used value, see Table I) the situation discussed before changes as it is depicted in Fig. 7.

In the beginning, when the temperature is still too cold for the regeneration process to occur, the occupation of states behaves almost similar as in the previous simulation (Fig. 6). Then, however, the simulations differ fundamentally. Without cooling it is not possible to reach a complete regeneration as the temperature rises too rapidly. Thus, in the case of a low regeneration rate, cooling the stack might become mandatory in order to facilitate a complete regeneration.

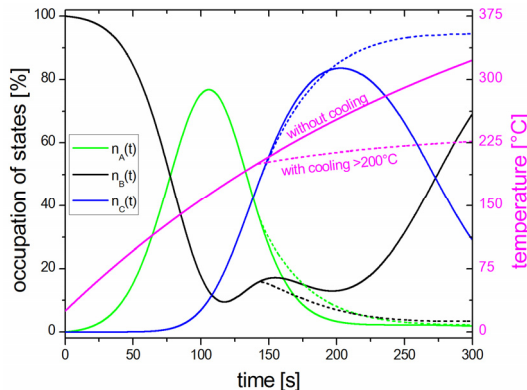


Figure 7: Exemplary simulation of the solar cell temperature profile resulting from power dissipation due to a constant current density of 75 mA/cm² and optional cooling for temperatures exceeding 200°C. Also shown is the occupation of states as reaction to the treatment. In this case a rather low regeneration rate was assumed.

4.4 Cooling considerations

As the simulations (Fig. 6 and Fig. 7) have shown, it has to be avoided that the stack heats itself beyond a certain temperature where the equilibrium does not favor the regenerated state any more as it is shown exemplarily in Fig. 2. Therefore, heat management becomes mandatory.

The development of the temperature T and its equilibrium ($dT/dt = 0$) may be described in principle by a heat conduction equation in the form

$$c \cdot \frac{dT}{dt} = P_{el}(T) - \gamma \cdot A \cdot (T - T_0)$$

with c being the heat capacity of the heated object, $P_{el}(T)$ the electrical losses, γ a rather complex heat exchange coefficient and A the area exposed to the surrounding material with temperature T_0 . Even though the equation is far too simple for the present geometry of the stacked solar cells, the principle dependencies are recognizable. The equilibrium temperature is reached when heat generation due to electrical losses is in balance with cooling. In the first experiment cooling was not very effective as the temperature rose by 50 K due to a relatively low current (even though this was chosen deliberately so that the target temperature was achieved). The stack was closely packed in that experiment thus the edge surface area per solar cell exposed to ambient was quite small (roughly 1 cm²).

However, the equation indicates what has to be done to achieve a better cooling and hence a lower net temperature even though the electrical losses (per cell) might be even higher (which is beneficial for regeneration). A key factor is to increase the area of the stack being in contact with the ambient, which means in first place to use spacers between the solar cells. Using spacers in the proof-of-principle experiment would have meant to increase the exposed area from roughly 1 cm² to around 300 cm² which is a tremendous gain. For 6'' solar cells (being thinner; $\sim 180 \mu\text{m}$) the gain changes from roughly 1 cm² to around 480 cm² but total power dissipation is also higher.

Using spacers between the solar cells has therefore a significant cooling effect even if cooling is only due to passive convective cooling. Arranging the stack vertically allows the warmed ambient to ascend between the solar cells drawing in cool ambient from below.

A further improvement, if necessary, is to increase the interaction volume of the ambient by circulation and thus to implement an active cooling system.

4.5 Cost assessment

Of course, in the context of mass production the question on the cost effectiveness of the presented technique arises. The whole system with handling etc. is hard to assess, however, the energy costs per cell may be estimated according to the simulations. As the heating is done only by the electrical self-heating of the stack and the regeneration process happens more or less casually at the same time, the needed energy can be calculated from the electrical losses integrated over time. In the simulation shown in Fig. 6 the regeneration is completed after 150 seconds and the temperature has risen almost linearly to 200°C. With a heat capacity c of the 6'' solar cell being around 8 J/K (assumed as 200 μm thick pure silicon wafer to simplify calculations), the required energy is approximately $c \times \Delta T = 8 \text{ J/K} \times 175 \text{ K} = 1.4 \text{ kJ}$. The integration yields a slightly higher value of 1.6 kJ due to the convex shape.

Thus the energy needed for the regeneration process depicted in Fig. 6 is roughly 1.6 kJ or 0.45 Wh per cell. This could be verified in an experiment yielding at most 2 Wh per cell or less. Assuming a rather conservative price of 0.15 €/kWh, the energy costs are around 0.07 € per thousand solar cells. So it can be stated here that energy costs are virtually negligible.

5. CONCLUSIONS

In this contribution it was shown that the regeneration process (a.k.a. permanent deactivation) of boron-oxygen related defects in solar cells can be carried out in a stack of solar cells (optionally separated by conductive spacers) which is externally biased. In this configuration a multitude of solar cells can be treated simultaneously. Besides inducing the regeneration process, the external biasing also brings along electrical losses and thus heats up the stack. This self-heating can be used to reach and/or hold the temperature required for the regeneration process.

In a proof-of-principle experiment the basic mode of operation could be successfully demonstrated, and, owing to the weak biasing, the regeneration process could also be successfully monitored in-situ.

However, simulations and experiments have shown that in-situ monitoring is challenging for stronger biasing as the degradation-regeneration cycle takes place during a phase of strong temperature increase covering up small differences in the applied voltage caused by the degradation and regeneration process.

As the simulations show, a complete regeneration might be achieved in a few minutes when high current densities are used. Of course, the current density can be chosen even higher than in the examples shown here accelerating the process even further as temperature rises quicker and the regeneration rate benefits from both higher temperatures and higher current densities. In addition, very strong biasing especially in the beginning can be used to rise the temperature to the desired range required for the regeneration process.

However, the simulations suggest that for high current densities a regulation of temperature or cooling might be necessary. For low current densities passive convective cooling of the stack is possible especially when conductive spacers are inserted between the solar cells. For higher current densities active cooling by intensified convection might be necessary.

The energy costs of regeneration in a stack triggered by external biasing were calculated showing that energy cost is more or less negligible.

6. REFERENCES

- [1] K. Bothe et al., Prog. Photovolt: Res. Appl. 2005, **13**: p.287
- [2] J. Schmidt et al., Proc. 29th IEEE PVSC, New Orleans, 2002
- [3] A. Herguth et al., Proc. 4th WCPEC, Waikoloa, 2006
- [4] A. Herguth et al., Prog. Photovolt: Res. Appl. 2008; **16**: p.135
- [5] J. Schmidt et al., Proc. 3rd WCPEC, Osaka, 2003
- [6] A. Herguth et al., Proc. 21st EU-PVSEC, Dresden, 2006
- [7] K. Bothe et al., J. Appl. Phys. **99**, 013701 (2006)
- [8] A. Herguth et al., J. Appl. Phys. **108**, 114509 (2010)